

# Different types of chaos in an optically injected semiconductor laser

Bernd Krauskopf<sup>a)</sup>

*Dept of Engineering Mathematics, University of Bristol, Bristol BS8 1TR, United Kingdom*

Sebastian Wiczorek and Daan Lenstra

*Department of Physics and Astronomy, Vrije Universiteit Amsterdam, De Boelelaan 1081, 1081 HV Amsterdam, The Netherlands*

(Received 14 April 2000; accepted for publication 18 July 2000)

With advanced tools from bifurcation theory routes to chaos via period doubling and the break-up of tori are identified. This allows us to distinguish between different types of chaos in terms of the output characteristics of the laser. We also find locking to a periodic solution inside a region of chaos. This information is important for applications requiring chaotic signals, such as encryption schemes. © 2000 American Institute of Physics. [S0003-6951(00)05737-5]

As complex nonlinear dynamics are of increasing interest for applications, such as cryptography<sup>1,2</sup> and computing,<sup>3</sup> the question arises to locate and study sources of chaotic output. Laser systems are natural candidates because they are indeed known to produce chaotic output and have the additional advantage of operating on very short time scales. Arguably the most accessible such laser system is a semiconductor laser subject to external optical injection. It is known that optical injection produces an enormous variety of phenomena, including chaotic output,<sup>4-8</sup> and the injection laser was recently considered for chaotic synchronization.<sup>9,10</sup>

An optically injected semiconductor laser is described well by the three-dimensional single-mode rate equation model<sup>8</sup>

$$\begin{aligned} \dot{E} &= K + (\frac{1}{2}(1 + i\alpha)n - i\omega)E, \\ \dot{n} &= -2\Gamma n - (1 + 2Bn)(|E|^2 - 1). \end{aligned} \tag{1}$$

Here  $E$  is the complex electric field,  $n$  is the population inversion,  $K$  is the injected field strength, and  $\omega$  the detuning of the injected field from the solitary laser frequency. Furthermore,  $\alpha$  is the linewidth enhancement factor,  $B$  is the cavity lifetime, and  $\Gamma$  is the damping rate. To keep this exposition simple we restrict to the case  $\alpha=2$ , but similar routes

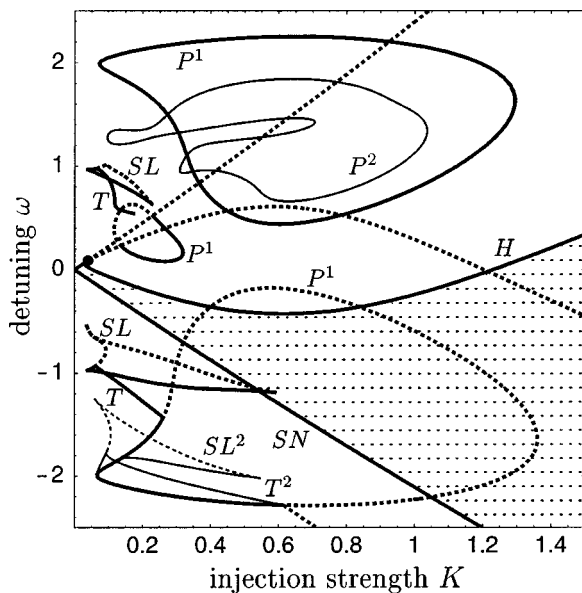


FIG. 1. The bifurcation diagram in the  $(K, \omega)$  plane. The stable locking region is shaded.

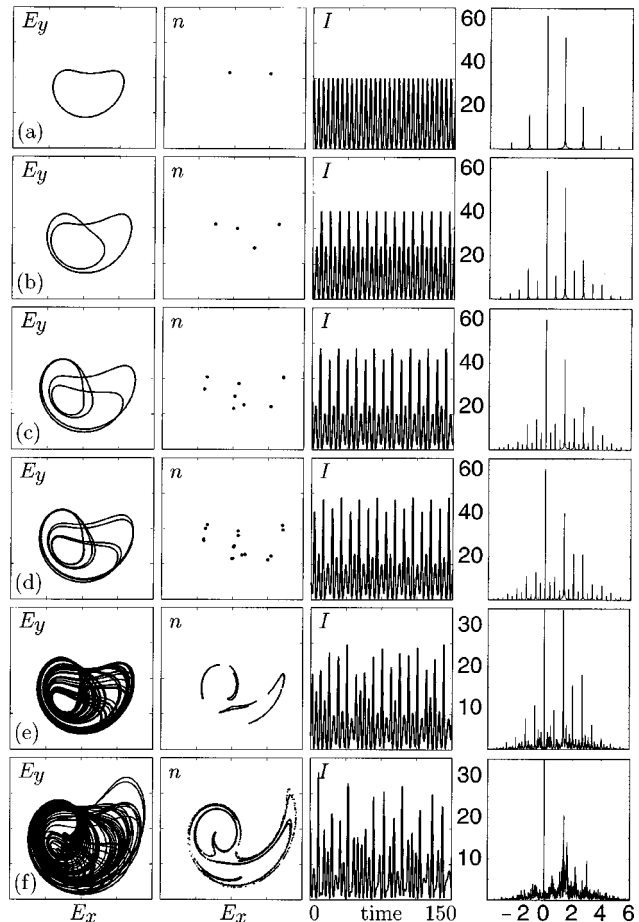


FIG. 2. Period-doubling route to chaos;  $K=0.62$  and from (a) to (f)  $\omega = 0.3, 0.5, 0.7, 0.71, 0.78,$  and  $1.1$ .

<sup>a)</sup>Electronic mail: B.Krauskopf@bristol.ac.uk

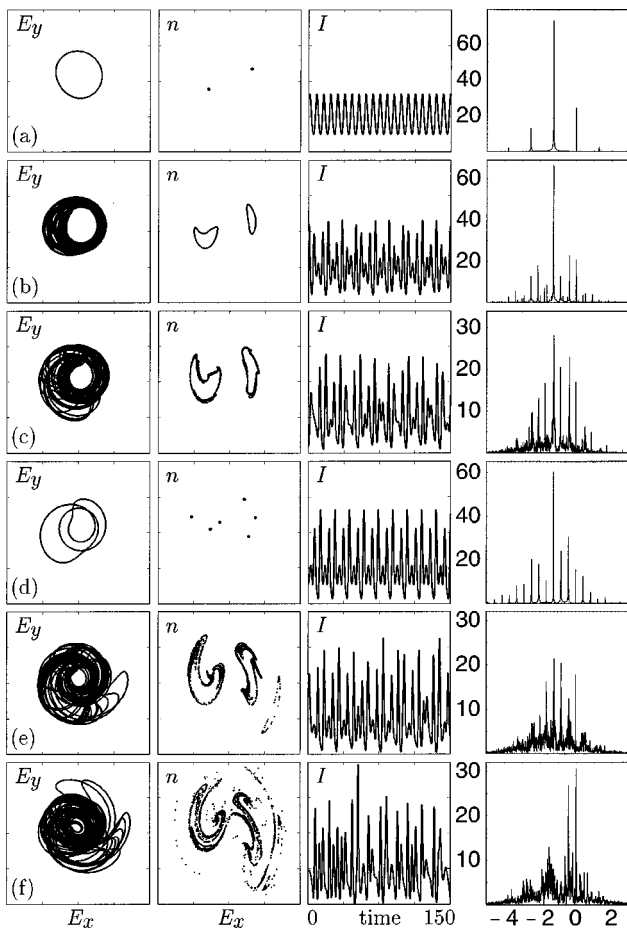


FIG. 3. Breakup of a torus;  $\omega = -1.2$  and from (a) to (f)  $K=0.15, 0.19, 0.23, 0.25, 0.29,$  and  $0.44$ .

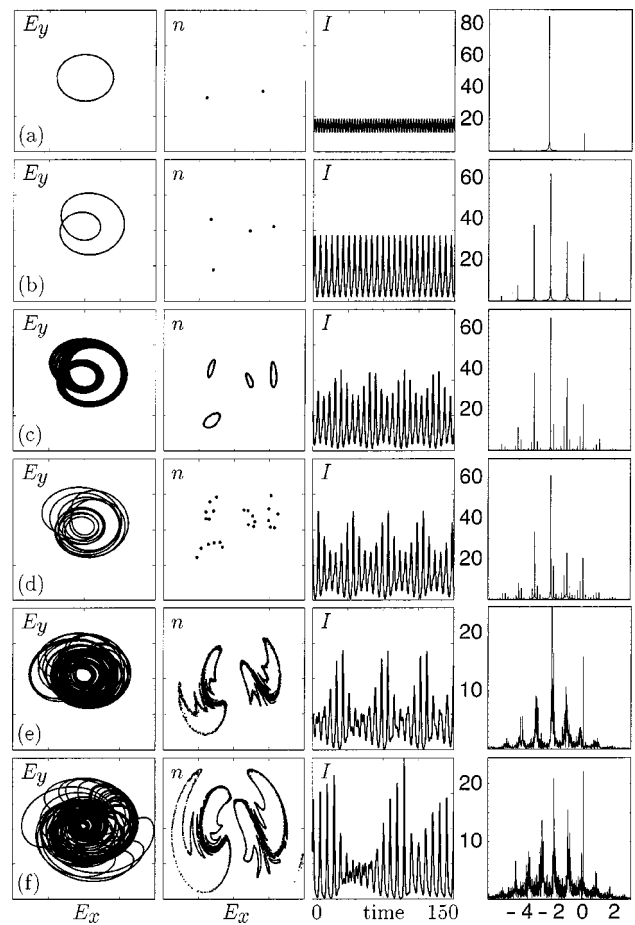


FIG. 4. Breakup of a period-two torus;  $K=0.23$  and from (a) to (f)  $\omega = -2.2, -2.0, -1.975, -1.96, -1.93,$  and  $-1.85$ .

chaos are present for different  $\alpha$  values.<sup>8</sup> Furthermore, we set  $B=0.015$  and  $\Gamma=0.035$ . The scaled variables and parameters in Eq. (1) can be related directly to experimental quantities.<sup>8</sup>

Figure 1 shows the bifurcation diagram of Eq. (1) in the  $(K, \omega)$  plane, consisting of saddle-node bifurcations (SN), Hopf bifurcations (H), period-doubling bifurcations (PD), saddle-node of limit cycle bifurcations (SL), and torus bifurcations (T). Bifurcations of stable objects are solid curves, and bifurcations of unstable objects are dashed curves. We only show the bifurcation curves that are relevant here. The bifurcation diagram is in good agreement with experimental and numerical studies,<sup>6,7</sup> but shows more detail so that different transitions to chaos can be studied.<sup>8</sup>

To to this end we take different paths through the bifurcation diagram in Fig. 1 and present the respective dynamics in four columns showing: the three-dimensional attractor of Eq. (1) projected onto the complex  $E$  plane, the attractor of the corresponding Poincaré map, the time series of the power, and the optical spectrum.

First we illustrate in Fig. 2 the well-known period-doubling route to chaos. An attracting periodic orbit (a) undergoes a sequence of period-doublings (b)–(d) until it apparently becomes chaotic (e) and (f). The attractor in (e) is already chaotic, and it shows a typical almost one-dimensional shape. Large peaks are present in the spectrum, so that it is hard to decide whether the spectrum is already broad. The attractor then grows further, the spectrum be-

comes broader, and the period-doubling peaks are less prominent, but still present (f). This involves further bifurcations not discussed here, such as interior crises.

An entirely different route to chaos is that via the break-up of a torus in Fig. 3. An attracting periodic orbit (a) loses its stability and a smooth attracting torus with quasi-periodic motion appears (b). Motion on a torus can be quasi-periodic or locked, and this is governed by resonance tongues. In general, a torus starts to break up when it is followed into a region where resonance tongues overlap. The smooth torus starts to lose its smoothness by forming self-similar protrusions (c) resulting in a chaotic attractor that is close to the original torus. Also in the spectrum, although it is broad, there is still much left of the previous dynamics. Embedded in the chaos we found a window with locking onto a period-three orbit (d). When the parameter is changed further the chaotic attractor reappears (e) and it becomes bigger (f) and does not resemble the original torus any longer. The spectrum broadens considerably (e) and then also loses the typical peaks of the torus dynamics (f). This transition to chaos is rather spectacular, and it results in a “much larger” chaotic attractor than can be found immediately after an accumulation of period doublings.

The two above transitions to chaos can occur in a mixed way. After a number of period-doublings one encounters a torus bifurcation, and the bifurcating torus of some higher base period then breaks up. An example of this is shown in Fig. 4. A periodic orbit (a) loses its stability and a period-two

orbit appears (b), which then bifurcates to an attracting torus (c) when the curve  $T^2$  in Fig. 1 is crossed. The power is modulated, but the frequencies of the period doubling are still prominent in the spectrum. The dynamics on the torus then locks to a period-six orbit (d). After the locking the torus is already breaking up (e). The ensuing chaotic attractor then grows, the power series becomes more chaotic and the spectrum even broader (f). Notice that there is still clear evidence of the frequencies that appeared in the period doubling.

In summary we identified and mapped out in detail different routes to chaos, exemplified by a sequence of period doublings, and the break-up of two different tori. The importance of this work lies in providing clear information of where certain types of chaotic dynamics can be found in a laser system that is experimentally quite accessible. In particular, we pointed out different output characteristics of the lasers, corresponding to chaotic attractors born in different ways. The chaotic attractor after period-doublings does not have a very broad spectrum and the frequency peaks typical for period doubling are still very prominent. These peaks disappear and the spectrum broadens only after further bifurcations leading to the growth of the attractor. On the other hand, the spectrum after the break-up of a torus appears to be quite broad. Here, a possible pitfall for applications is the occurrence of locking on the broken-up torus. We found a loss of chaos over a certain parameter range due to locking onto a period-three orbit. We expect this to be observable in experiments.

The variability of chaotic attractors presented here is important for applications requiring a chaotic signal with particular properties. For example, for chaotic encryption schemes where the parameter values provide the encryption key<sup>10</sup> one needs to be confident to switch between suitable types of chaos. A loss of chaos due to locking must be avoided to ensure privacy. Investigating this further remains an interesting challenge for future research.

The research of S.M.W. was supported by the Foundation for Fundamental Research on Matter (FOM), which is financially supported by the Netherlands Organization for Scientific Research (NWO). B.K. thanks the British Council and NWO for support under the UK-Dutch Joint Scientific Research Programme.

<sup>1</sup>G. D. Van Wiggeren and R. Roy, *Science* **279**, 1198 (1997).

<sup>2</sup>C. R. Mirasso, P. Colet, and P. Garcia-Fernández, *IEEE Photonics Technol. Lett.* **8**, 299 (1996).

<sup>3</sup>S. Sinha and W. L. Ditto, *Phys. Rev. Lett.* **81**, 2156 (1998).

<sup>4</sup>L. A. Lugiato, L. M. Narducci, D. K. Bandy, and C. A. Pennise, *Opt. Commun.* **46**, 64 (1983).

<sup>5</sup>J. R. Tredicce, F. T. Arecchi, G. L. Lippi, and G. P. Puccioni, *J. Opt. Soc. Am. B* **2**, 173 (1985).

<sup>6</sup>V. Kovanis, A. Gavrielides, T. B. Simpson, and J. M. Liu, *Appl. Phys. Lett.* **67**, 2780 (1995).

<sup>7</sup>T. B. Simpson, J. M. Liu, K. F. Huang, and K. Tai, *Quantum Semiclass. Opt.* **9**, 765 (1997).

<sup>8</sup>S. M. Wieczorek, B. Krauskopf, and D. Lenstra, *Opt. Commun.* **172**, 279 (1999).

<sup>9</sup>V. Annovazzi-Lodi, S. Donati, and A. Scire, *IEEE J. Quantum Electron.* **32**, 953 (1996).

<sup>10</sup>H. F. Chen and J. M. Liu, *IEEE J. Quantum Electron.* **36**, 27 (2000).